ENCIT 2018

ABCM Associação Brasileira de Engenharia e Ciências Mecânicas

17th Brazilian Congress of Thermal Sciences and Engineering
November 25th-28th, 2018, Águas de Lindóia, SP, Brazil

ENCIT-2018-XXXX
CFD SIMULATION OF SUBCOOLED FLOW BOILING IN A COOLANT SUBCHANNEL OF A PWR

Felipe P. Ribeiro
Jian Su
Nuclear Engineering Department, COPPE-POLI
Universidade Federal do Rio de Janeiro
Av. Horácio Macedo, 2030, G206, Centro de Tecnologia, Cidade Universitária,
21941-914 Rio de Janeiro, Brazil
felipeportor@poli.ufrj.br
sujian@nuclear.ufrj.br

Abstract.
Two-phase flows can be found in a wide variety of industrial applications, so understanding the process of phase change is of crucial importance for the operation and safety of many industrial equipment, including nuclear reactor. The high capacity of Computational Fluid Dynamics (CFD) code to predict multi-dimensional thermal-hydraulics behavior and multiphase flows, allied to the increased availability of capable computer systems, are making CFD a good tool to simulate single and two-phase phenomena of thermal-hydraulics nature in nuclear reactors. The present work proposes a study of subcooled flows to better understand the Eulerian RPI (Rensselaer Polytechnic Institute) wall boiling model and its closure models, existing in the commercial code ANSYS - Fluent, through analyses of mesh refinement and turbulence model impact on this model. Numerical results of CFD simulation compare favorably with available numerical and experimental data.

Keywords: *CFD, RPI, Subcooled, Boiling*

1. INTRODUCTION

In the nuclear industry, pressurized water reactors operate in a high pressure, avoiding boiling of primary coolant. However, the production of located small quantities of bubbles at the wall of fuel rods is acceptable, which characterize the regime of subcooled flow. To ensure the safety of nuclear reactor, it is important to well understand the phase change in this environment.

Computational fluid dynamics (CFD) method is a good tool to simulate multiphase thermal-hydraulics phenomena, as well as phase change, due to the wide rage of experimental correlations implemented in these commercial codes, including ANSYS - Fluent. Combined with the increasing of computational capacity, CFD is becoming a good tool to increase the accuracy of nuclear safety analyses, helping people to better understand the physical phenomena in those systems.

The Eulerian RPI (Rensselaer Polytechnic Institute) wall boiling model, already implemented in Fluent, has been chosen as the phase change model for the simulations based in observations of Gu *et al.* (2017) and Filho *et al.* (2016). This model is initially presented in the present paper with a brief review of mathematical models used by the CFD code. After that, two 2D axisymmetric cylindrical geometry, well documented in literature (after experiments of Bartolomei and Chanturiya (1967)), are presented with a mesh convergence study.

In this work, the main objective is to understand the use and implementation of RPI wall boiling model in Fluent and evaluate the impact of mesh fineness, different turbulence models and closure models on a subcooled flow.

Once Fluent RPI model have been well understood, it will be applied in future works to the coupled neutron kinetics-thermal-hydraulics model with continuous feedback previously developed in Ribeiro (2017), given the capacity to perform dynamic analyses of a PWR subchannel during disturbances and accident scenarios with boiling of the primary coolant.

2. MATHEMATICAL MODELS AND METHODS

Two 2D axisymmetric cylindrical geometries have been developed allowing the study of impact of the RPI wall boiling model in a subcooled flow. The simulation of the mathematical model includes the continuity equation, momentum equation, and energy equation for each phase, and k-ϵ and k-ω SST turbulence models.

2.1 Conservation equations

Continuity equation:

$$\frac{\partial}{\partial t}(\alpha_i \rho_i) + \nabla.(\alpha_i \rho_i \mathbf{u}_i) = S_i + \dot{m}_{ji} - \dot{m}_{ij}. \tag{1}$$

Momentum equation:

$$\frac{\partial}{\partial t}(\alpha_i \rho_i \mathbf{u}_i) + \nabla.(\alpha_i \rho_i \mathbf{u}_i \mathbf{u}_i) = -\alpha_i \nabla p + \nabla.\overline{\overline{\tau}}_i + \alpha_i \rho_i \mathbf{g} + \dot{m}_{ji}\mathbf{u}_j - \dot{m}_{ij}\mathbf{u}_i + \mathbf{F}_{D,i} + \mathbf{F}_{L,i} + \mathbf{F}_{wl,i} + \mathbf{F}_{td,i} + \mathbf{F}_{vm,i}. \tag{2}$$

Energy equation:

$$\frac{\partial}{\partial t}(\alpha_i \rho_i h_i) + \nabla.(\alpha_i \rho_i \mathbf{u}_i h_i) = \alpha_i \frac{\partial p_i}{\partial t} - \nabla.\mathbf{q}_i + S_i + Q_{ij} + \dot{m}_{ji}h_j - \dot{m}_{ij}h_i, \tag{3}$$

where α_i, ρ_i, $\mathbf{u}_i$, S_i, p_i, $\overline{\overline{\tau}}_i$, h_i and $\mathbf{q}_i$ denote, respectively, the volume fraction, density, velocity, source term, pressure, stress tensor, specific enthalpy and heat flux for phase *i*. Q_{ij} and $\dot{m}_{ij}$ are the energy and mass transfer from phase *i*th to *j*th. And $\mathbf{F}_{D,i}$, $\mathbf{F}_{L,i}$, $\mathbf{F}_{wl,i}$, $\mathbf{F}_{td,i}$ and $\mathbf{F}_{vm,i}$ are, respectively, the drag force, lift force, wall lubrification force, turbulence dispersion force and virtual mass force.

2.2 k-ϵ turbulence model

The standard k-ϵ model is a two equations model, derived from Reynolds-averaged Navier-Stokes equations (RANS), based on model transport equations for the turbulence kinetic energy, k, and its dissipation rate, ϵ.

Turbulence kinetic energy, k:

$$\frac{\partial(\rho k)}{\partial t} + \frac{\partial(\rho k u_i)}{\partial x_i} = \frac{\partial}{\partial x_j}\left(\frac{\mu_t}{\sigma_k}\frac{\partial k}{\partial x_j}\right) + 2\mu_t E_{ij}E_{ij} - \rho\epsilon. \tag{4}$$

Turbulent dissipation rate, ϵ:

$$\frac{\partial(\rho \epsilon)}{\partial t} + \frac{\partial(\rho \epsilon u_i)}{\partial x_i} = \frac{\partial}{\partial x_j}\left(\frac{\mu_t}{\sigma_\epsilon}\frac{\partial \epsilon}{\partial x_j}\right) + C_{1\epsilon}\frac{\epsilon}{k}2\mu_t E_{ij}E_{ij} - C_{2\epsilon}\rho\frac{\epsilon^2}{k}, \tag{5}$$

where $C_{1\epsilon}$ and $C_{2\epsilon}$ are constants, E_{ij} is the deformation rate and μ_t is the turbulent viscosity:

$$\mu_t = \rho C_\mu \frac{k^2}{\epsilon}, \tag{6}$$

where C_μ is a constant.

2.3 k-ω SST turbulence model

The k-ω SST model is a two equations hybrid model that solves near-wall flows using the k-ω model and the fully turbulent development region using the k-ϵ model. Its equations are also derived from RANS equations and can be described as follows (Vieira, 2014).

Turbulence kinetic energy, k:

$$\frac{\partial k}{\partial t} + \overline{u_j}\frac{\partial k}{\partial x_j} = \frac{\partial}{\partial x_j}\left[\left(\nu + \nu_t\left(\frac{1}{F_1^{-1}\sigma_{k1}} + \frac{1}{(1-F_1)^{-1}\sigma_{k2}}\right)\right)\frac{\partial k}{\partial x_j}\right] + P_k\frac{\partial \overline{u_i}}{\partial x_j} - \beta_k k\omega, \tag{7}$$

Specific dissipation rate, ω:

$$\begin{aligned}\frac{\partial \omega}{\partial t} + \overline{u_j}\frac{\partial \omega}{\partial x_j} &= \frac{\partial}{\partial x_j}\left[\left(\nu + \nu_t\left(\frac{1}{F_1^{-1}\sigma_{\omega1}} + \frac{1}{(1-F_1)^{-1}\sigma_{\omega2}}\right)\right)\frac{\partial \omega}{\partial x_j}\right] \\ &+ (1-F_1)\frac{2}{\sigma_{\omega2}\upsilon}\left(\frac{\partial k}{\partial x_j}\frac{\partial \omega}{\partial x_i}\right) - \left[F_1\beta_{\omega1} + (1-F_1)\beta_{\omega2}\right]\omega^2 + \left[F_1\alpha_1 + (1-F_1)\alpha_2\right]\frac{\omega}{k}P_k,\end{aligned} \tag{8}$$

where

$$P_k = \nu_t \left(\frac{\partial \overline{u_i}}{\partial x_j} + \frac{\partial \overline{u_j}}{\partial x_i} \right) - \frac{2}{3} \kappa \delta_{ij}, \tag{9}$$

and the turbulence viscosity is given by

$$\nu_t = \frac{\alpha k}{\max(\alpha\omega, SF_2)}, \tag{10}$$

where S is an invariant measure of strain rate.

2.4 RPI wall boiling model

The RPI wall boiling model was developed to model the energy directly transferred from the wall to the fluid. In this model, the total heat flux, from the heated wall to the working fluid, is partitioned into three components: the convective heat flux (q_C), the quenching heat flux (q_Q) and the evaporative heat flux (q_E).

$$q_W = q_C + q_Q + q_E. \tag{11}$$

The convective heat flux can be expressed as:

$$q_C = h_C(T_w - T_i)(1 - A_b), \tag{12}$$

where h_C is the single phase turbulent heat transfer coefficient, T_w and T_i are, respectively, the wall and fluid temperatures and A_b is the proportion of heated wall covered by nucleating bubbles:

$$A_b = min\left(1, K\frac{N_w \pi D_w^2}{4}\right), \tag{13}$$

where K is an empirical constant:

$$K = 4.8e^{-\frac{Ja_{sub}}{80}} \tag{14}$$

and Ja_{sub} is the subcooled Jacob number:

$$Ja_{sub} = \frac{\rho_l C_{pl} \Delta T_{sub}}{\rho_v h_{lv}}, \tag{15}$$

where ΔT_{sub} is the liquid subcooling, C_{pl} is the specific heat of liquid, ρ_l and ρ_v are, respectively, liquid and vapor density and h_{lv} is the latent heat of evaporation.

The quenching heat flux can be expressed as:

$$q_Q = \frac{2k_l}{\sqrt{\pi \lambda_l \tau}} A_b (T_w - T_i), \tag{16}$$

where k_l is the thermal conductivity of liquid phase, τ is the periodic time and λ_l is the difusivity.

The evaporative heat flux can be expressed as:

$$q_E = V_d N_w f \rho - v h_{lv}, \tag{17}$$

where V_d is the bubble volume based on the bubble departure diameter.

2.5 Closure models for the RPI wall boiling model

The calculation of the heat flux components, q_C, q_Q and q_E, depends on the characteristics of bubble nucleation, growth, and departure in the subcooled flow boiling process. The most important parameters of the RPI wall boiling model are the active nucleation site density (N_w), bubble departure diameter (D_w) and bubble departure frequency (f). However, these parameters cannot be theoretically derived because of the complex physics of wall boiling, closely related to the wall surface properties. Therefore, a series of empirical correlations have been proposed.

Two models for the active nucleation site density (N_w) were used in this work. The first one was proposed by Kocamustafaogullari and Ishii (1983). When applying the correlation to forced convective nucleate boiling, an effective superheat is used to replace the actual superheat in the model, as:

$$N_w = \frac{f(\rho*)}{D_w^2}\left(\frac{4\sigma T_{sat}}{\rho_g h_{lv} D_w \Delta T_e}\right)^{-4.4}, \tag{18}$$

where T_{sat} is the saturated temperature, ΔT_e is an effective superheat and $f(\rho*)$ is a function of the density:

$$f(\rho*) = 2.157x10^{-7}(\rho*)^{-3.2}(1+0.0049\rho*)^{4.13}, \tag{19}$$

with $\rho* = \frac{(\rho_l - \rho_v)}{\rho_v}$.

The second N_w model was proposed by Lemmert and Chawla (1977) while investigating pool boiling of saturated water. It can be described as:

$$N_W = C^n \left(T_W - T_{sat}\right)^n, \tag{20}$$

where n and C are empirical parameters, assumed as 1.805 and 210, respectively, based on recomendations made by Kurul and Podowski (1991).

Forces acting on a bubble reach the balance state when the bubble starts to detach from the surface, allowing correlation to be derived based on such balance. Bubble departure diameter (D_w) is a function of contact angle, thermal properties and the mass flux. This work also uses two models for the departure diameter. The first one was developed by Kocamustafaogullari and Ishii (1983):

$$D_w = 0.0012\left(\frac{(\rho_l - \rho_v)}{\rho_v}\right)^{0.9}\left[0.0208\phi\sqrt{\frac{\sigma}{g(\rho_l - \rho_v)}}\right], \tag{21}$$

where σ is the surface tension and ϕ is the contact angle in degrees.

In equation 21, prefix factors are used to reduce the dependence of D_w on the liquid / vapor density ratio at higher pressures.

The second D_w model used in this work was developed by Unal (1976) while doing experiments to establish correlations to the growth rate. The model considers that if the bubble does not collapse it will departs from the wall after reaching a maximum size.

$$D_w = 2,421x10^{-5}p^{0,709}\left(\frac{a}{b\sqrt{\phi}}\right), \tag{22}$$

where $a = \frac{\Delta T_{sup}}{2\rho_g h_{lv}}\sqrt{\frac{\rho_w C_{pw} k_w}{\pi}}$.

If $\Delta T_{sub} \leq 3$:

$$b = \frac{\Delta T_{sub}}{2\left(1 - \frac{\rho_v}{\rho_l}\right)} e^{\left(\frac{\Delta T_{sub}}{3} - 1\right)}, \tag{23}$$

If $\Delta T_{sub} > 3$:

$$b = \frac{\Delta T_{sub}}{2\left(1 - \frac{\rho_v}{\rho_l}\right)}, \tag{24}$$

and

$$\phi = max\left(\left(\frac{U_b}{U_0}\right)^{0,47}; 1, 0\right). \tag{25}$$

where p is the operational pressure, $T_{sub} = T_W - T_{sat}$ is the wall superheat, U_b is the flow velocity near the wall and $U_0 = 0,61m/s$.

Departure frequency (f) denotes, in subcooled boiling process, the cycle of bubble generation, growth to the size D_w and detaching from the wall at one given nucleation site. The widely used correlation, also used in this work, was developed by Cole (1960):

$$f = \sqrt{\frac{4g(\rho_l - \rho_v)}{3\rho_l D_w}}. \tag{26}$$

2.6 CFD model

In order to reduce computational costs, the subcooled model can be reduced to a 2D axisymmetric model, shown by figure 1.

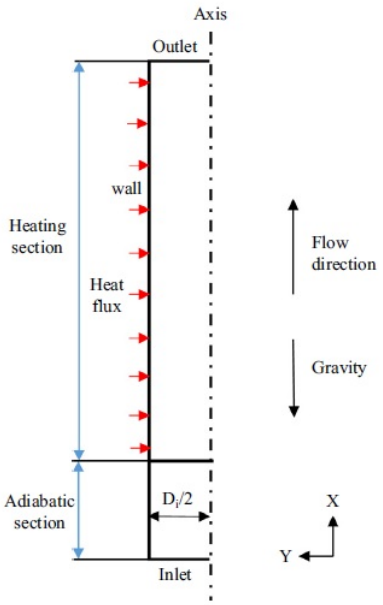

Figure 1: **2D axisymmetric geometry (Gu *et al.*, 2017).**

With the objective of validating the Eulerian RPI model for future uses, numerical simulations were conducted using two combinations of geometries and conditions of experimental studies of Bartolomei and Chanturiya (1967) and G G Bartolomei and Mikhailov (1982).

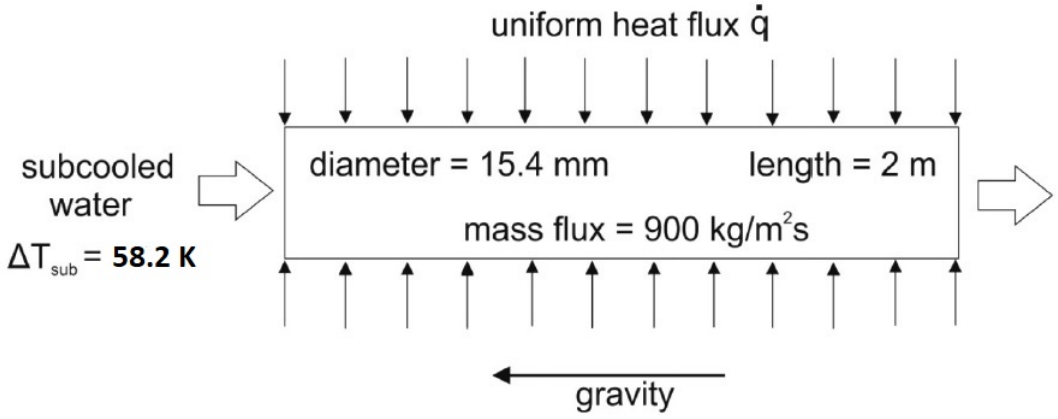

Figure 2: **Simulation domain and boundary conditions for case A (Filho *et al.* (2016) - adapted).**

Figure 1 shows the geometry used for simulations of case A (see table 1). Although the cylinder is represented as a 2D geometry, an axisymmetric model was used for all subcooled simulations.

For simulations of case B, a 2D axisymmetric model of a cylinder with inner diameter of 12.0 mm and length of 1.5 m was used.

Table 1: **Initial and boundary conditions for the subcooled model.**

Parameter	Case A	Case B
Operational pressure (MPa)	4.50	6.81
Inlet temperature (K)	472.39	521.00
Saturation temperature (K)	530.59	557.12
Wall heat flux (kW/m^2)	570.00	440.00
Mass flux (kg/m^2)	900.00	998.00

Properties of liquid water (first phase) phase were considered variables (compressible flow) according to the piecewise-linear interpolation method. However, for proper treatment of the two-phase flow with phase change using a CFD code, properties of the vapor (second phase) phase were considered constant, as well as its temperature, constant at the saturation temperature (T_{sat} = 530.59 K).

Two different combinations of closure models were chosen based on Gu *et al.* (2017) study:

Table 2: **Closure models combinations.**

Combination	N_W Model	D_W Model	f Model
C1	Lemmert-Chawla	Unal	Cole
C2	Kocamustafaogullari-Ishii	Kocamustafaogullari-Ishii	Cole

3. RESULTS

The study of subcooled flows at the present work focuses on the influence of mesh finesses and turbulence models on the RPI wall boiling model. Therefore, results for the k-ϵ and k-ω SST turbulence models are compared to results from Gu *et al.* (2017) using the mesh with better commitment between precision and calculation velocity. All simulations use case A from table 1, except when indicated.

3.1 k-ϵ model

A mesh sensitivity study for the cylindrical axysimmetric geometry was performed using the k-ϵ standard turbulence model.

Table 3 shows the influence of mesh refinement on the vapor void fraction at outlet for five different meshes.

Table 3: **Mesh sensivity study for k-ϵ model.**

Mesh number	Radial refinement	Axial refinement	Number of nodes	Vapor void fraction
01	10	95	950	0.509
02	15	110	1650	0.506
03	20	125	2500	0.504
04	25	140	3500	0.504
05	30	155	4650	0.504

Based on the results presented by table 3 and figures 3a and 3b, mesh number 03 can be chosen as the best mesh.

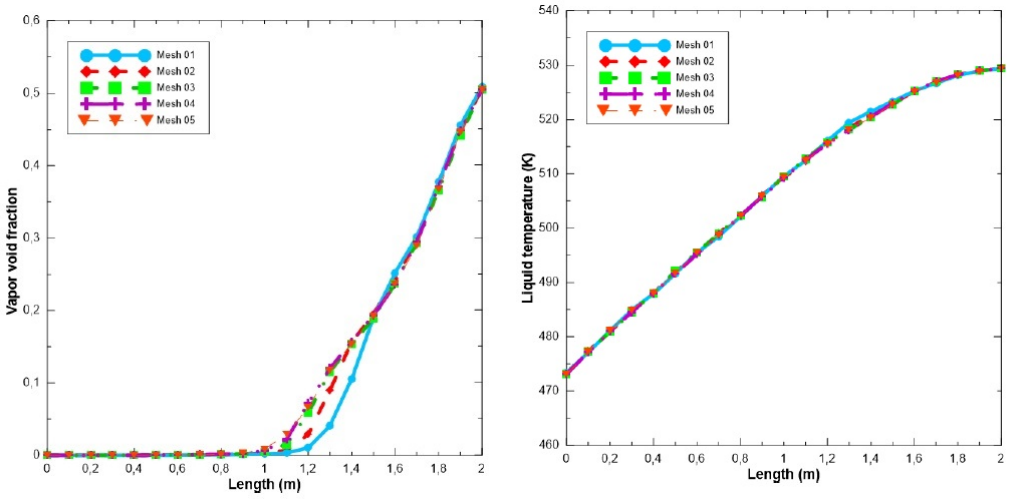

(a) (b)

Figure 3: **Mesh sensitivity study using k-ϵ model: (a) vapor void fraction behavior; (b) Liquid temperature behavior.**

3.2 k-ω SST model

Using the same geometry, a mesh sensitivity study was performed with the k-ω SST turbulence model. Table 4 shows the influence of mesh refinement on the vapor void fraction at outlet for four different meshes.

Table 4: **Mesh sensivity study for k-ω SST model.**

Mesh number	Radial refinement	Axial refinement	Number of nodes	Vapor void fraction
01	10	95	950	0.510
02	15	110	1650	0.513
03	20	125	2500	0.514
04	20	1250	25000	0.514

A comparison between these four meshes through table 4 and figures 4a and 4b allows us to choose mesh number 03 for further calculations and shows the independence of axial refinement (see meshes number 03 and 04), due to the predominance of axial behavior of subcooled boiling.

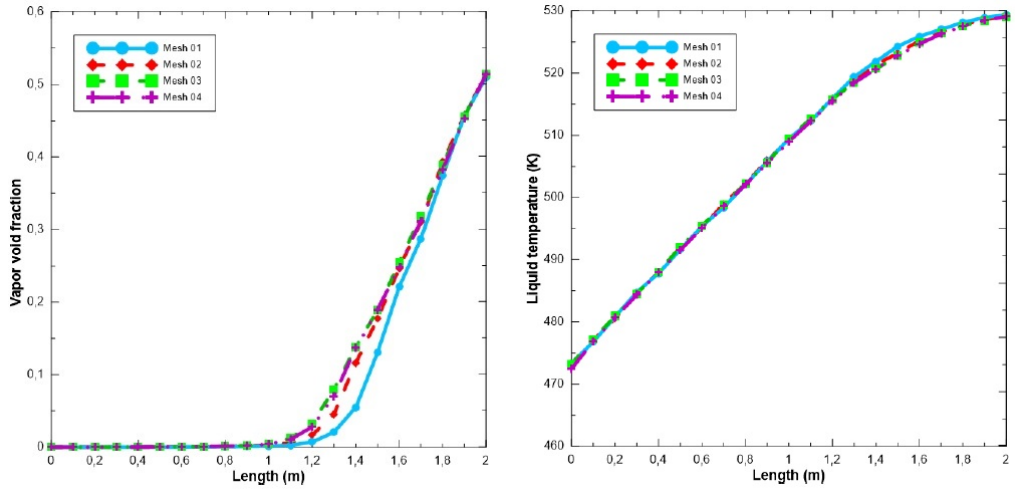

(a) (b)

Figure 4: **Mesh sensitivity study using k-ω SST model: (a) vapor void fraction behavior;(b) Liquid temperature behavior.**

Using both chosen meshes (one for each turbulence model), results of simulations with k-ϵ and k-ω SST turbulence

models can be compared to numerical results obtained by Gu *et al.* (2017). Table 5, figure 5 and 6 summarize this analysis.

Table 5: **Comparison of numerical results.**

Parameter	Gu *et al.* (2017)	Fluent k-ϵ	Fluent k-ω SST
T_{sat} (K)	530.59	530.59	530.59
T_{sub} (K)	58.20	58.20	58.20
T_{in} (K)	472.39	472.39	472.39
T_{max} wall (K)	-	544.17	544.03
T_{max} liquid (K)	-	530.42	530.22
Vapor vol. fraction at outlet	0.49	0.50	0.51
Beginning of boiling (m)	1.00	1.00	1.00

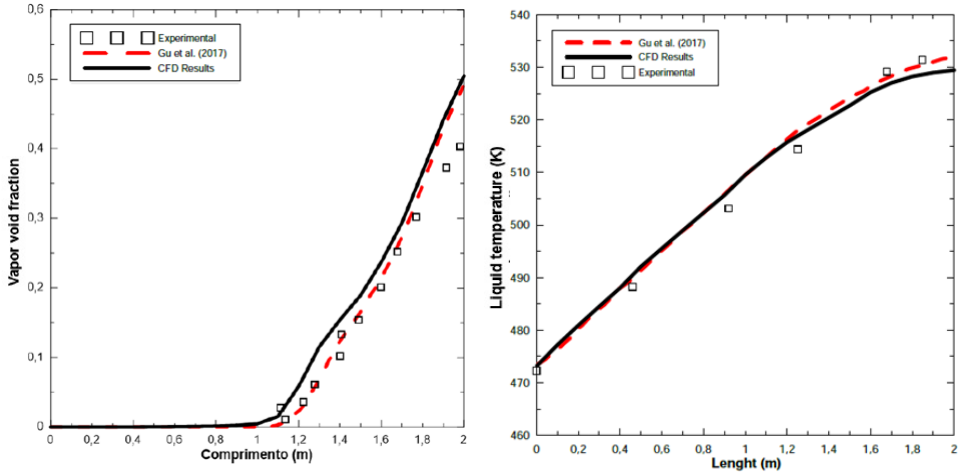

(a) (b)

Figure 5: **Comparison of numerical results using k-ϵ model: (a) vapor void fraction; (b) liquid temperature.**

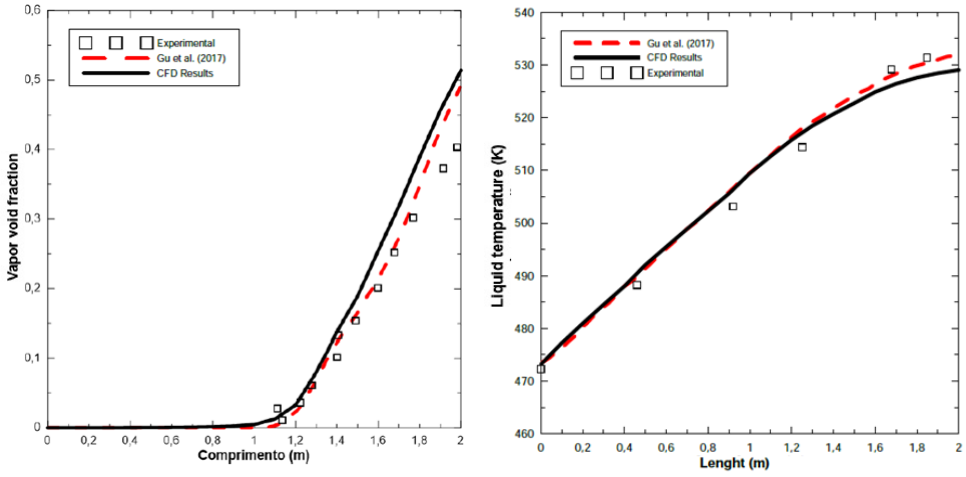

(a) (b)

Figure 6: **Comparison of numerical results using k-ω SST model: (a) vapor void fraction; (b) liquid temperature.**

The k-ω SST model is adopted for further calculations, as it presents similar results to Gu *et al.* (2017) and there are no significant difference between turbulence models and k-ω SST. It will be convenient to implement the RPI wall boiling model into the coupled neutronic-thermal-hydraulics model previously developed, which also uses k-ω SST turbulence model.

Figure 9 shows the vapor void fraction (or volume fraction) at the last quarter of the 2D cylindrical geometry for the mesh number 03 of k-ω SST model mesh sensitivity study. Using this turbulence model, it is possible to see how vapor begins to be formed at the heat wall until occupying the whole flow with vapor void fraction up to 0.50 at outlet.

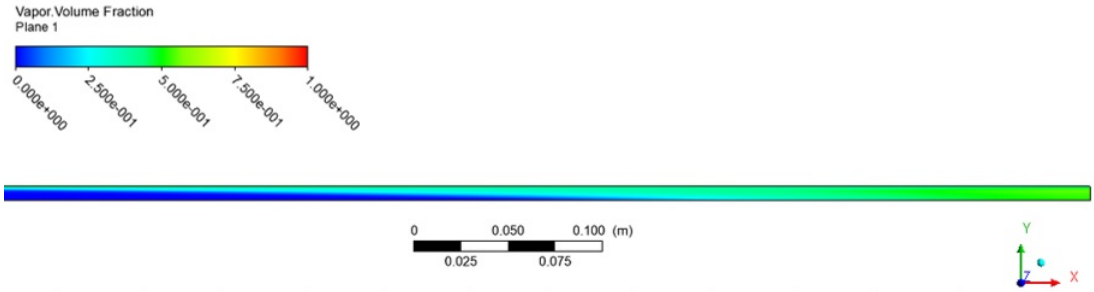

Figure 7: **Vapor void fraction axial distribution.**

3.3 Closure models for the RPI wall boiling model

A comparison between different combinations of closure models (see table 2) was performed to establish the best combination against experimental data.

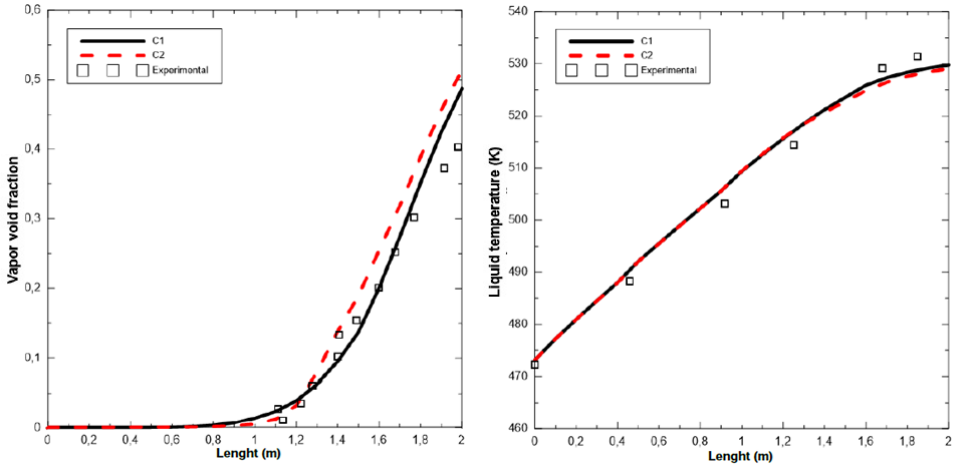

(a) (b)

Figure 8: **Comparison of numerical results using closure models combinations from table 2: (a) vapor void fraction; (b) liquid temperature.**

3.4 Simulation of case B

Using the k-ω SST model and the specific geometry for case B, but with same mesh discretization from mesh number 03 (previously validated for case A), this case was simulated showing the influence of different mass flux and operational pressure on the model.

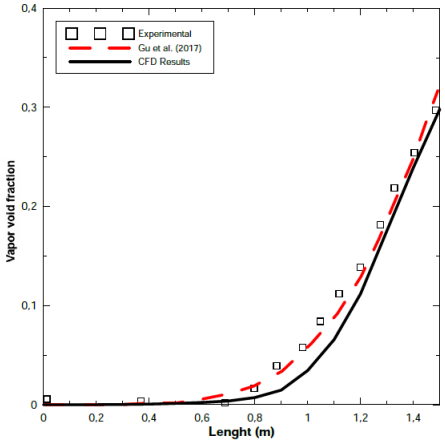

Figure 9: **Axial vapor void fraction for case B.**

4. CONCLUSIONS

The present work presents a study of Fluent Eulerian RPI wall boiling model which was able to demonstrate the influence of turbulence model and mesh fineness in fluid temperature and vapor void fraction. The obtained results, in accordance with literature numerical and experimental data, show the correct implementation of this model for two-phase flows with phase change, for different mass fluxes and operational pressures.

A comparison of different combinations of closure models for the RPI wall boiling models shows that the combination C1 from table 2 matches better with experimental data and can be used in a wide application scope.

For future works, in order to study the core behavior during scenarios of boiling of the primary coolant, RPI model should be implemented together with the neutron kinetics-thermal-hydraulics coupled model with feedback reactivity, previously developed (Ribeiro (2017)), to predict two-phase flows behavior in nuclear reactors safety analyses in agreement with power generation in the fuel.

5. ACKNOWLEDGEMENTS

The authors acknowledge gratefully the financial support from Brazilian funding agencies: CNPq, FAPERJ, and CAPES.

6. REFERENCES

Bartolomei, G.G. and Chanturiya, V.M., 1967. "Experimental study of true void fraction when boiling subcooled water in vertical tubes". In *Thermal Engineering*. Vol. 14, pp. 123–128.

Cole, R., 1960. "A photographic study of pool boiling in the region of the critical heat flux". In *AIChE J.* Vol. 4, pp. 533–538.

Filho, F.A.B., Ribeiro, G.B. and Caldeira, A.D., 2016. "Prediction of subcooled flow boiling characteristics using two-gluid eulerian cfd model". In *Nuclear Engineering and Design*. Vol. 308, pp. 30–37.

G G Bartolomei, V.G.B. and Mikhailov, V.N., 1982. "An experimental investigation true volumetric vapor content with subcooled boiling in tubes". In *Thermal Engineering*. Vol. 29, pp. 132–135.

Gu, J., Wang, Q., Wu, Y., Lyu, J., Li, S. and Yao, W., 2017. "Modeling of subcooled boiling by extending the rpi wall boiling model to ultra-high pressure conditions". In *Applied Thermal Engineering*. Vol. 124, pp. 571–584.

Kocamustafaogullari, G. and Ishii, M., 1983. "Interfacial area and nucleation site dendity in boiling systems". In *Int. J. Heat Transfer*. Vol. 9, pp. 1377–1387.

Kurul, N. and Podowski, M.Z., 1991. "On the modeling of multidimensional effects in boiling channels". In *Proceedings of the 27th national heat transfer conference*. pp. 301–314.

Lemmert, M. and Chawla, J.M., 1977. "Influence of flow velocity on surface boiling heat transfer coefficient". In *Heat Transfer in Boiling*. pp. 237–247.

Ribeiro, F.P., 2017. "Simulação cfd com acoplamento neutrônico de um subcanal de um pwr com condições de inserção de reatividade e parada de bomba". In *Ecola Politécnica /UFRJ*.

Unal, H.C., 1976. "Maximum bubble diameter, maximum bubble-growth time and bubble-growth rate during the subcooled nucleate flow boiling of water up to 17.7 mn/m2". In *Int. J. Heat Mass Transfer*. Vol. 19, pp. 643–649.

Vieira, C.B., 2014. "Simulação computacional de convecção natural turbulenta em cavidades com geração de calor volumétrica". In *COPPE/UFRJ*.

7. RESPONSIBILITY NOTICE

The authors are the only responsible for the printed material included in this paper.